Molecular Cancer Therapeutics

Preclinical Development

Humanization of an Anti-CCR4 Antibody that Kills Cutaneous T-Cell Lymphoma Cells and Abrogates Suppression by T-Regulatory Cells

De-Kuan Chang[1,2], Jianhua Sui[1,2], Shusheng Geng[1,2], Asli Muvaffak[1], Mei Bai[3], Robert C. Fuhlbrigge[3], Agnes Lo[1], Anuradha Yammanuru[1], Luke Hubbard[1], Jared Sheehan[1], James J. Campbell[3], Quan Zhu[1,2], Thomas S. Kupper[3], and Wayne A. Marasco[1,2]

Abstract

Cutaneous T-cell lymphoma (CTCL) is a heterogeneous group of neoplastic disorders characterized by clonally derived and skin-homing malignant T cells that express high level of chemokine receptor CCR4, which is associated with their skin-homing capacity. CCR4 is also highly expressed on T-regulatory cells (Tregs) that can migrate to several different types of chemotactic ligand CCL17- and CCL22-secreting tumors to facilitate tumor cell evasion from immune surveillance. Thus, its high-level expression on CTCL cells and Tregs makes CCR4 a potential ideal target for antibody-based immunotherapy for CTCL and other types of solid tumors. Here, we conducted humanization and affinity optimization of a murine anti-CCR4 monoclonal antibody (mAb), mAb1567, that recognizes both the N-terminal and extracellular domains of CCR4 with high affinity and inhibits chemotaxis of $CCR4^+$ CTCL cells. In a mouse CTCL tumor model, mAb1567 exhibited a potent antitumor effect and *in vitro* mechanistic studies showed that both complement-dependent cytotoxicity (CDC) and neutrophil-mediated antibody-dependent cellular cytotoxicity (ADCC) likely mediated this effect. mAb1567 also exerts human NK cell–mediated ADCC activity *in vitro*. Moreover, mAb1567 also effectively inhibits chemotaxis of $CD4^+CD25^{high}$ Tregs *via* CCL22 and abrogates Treg suppression activity *in vitro*. An affinity-optimized variant of humanized mAb1567, mAb2-3, was selected for further preclinical development based on its higher binding affinity and more potent ADCC and CDC activities. Taken together, this high-affinity humanized mAb2-3 with potent antitumor effect and a broad range of mechanisms of action may provide a novel immunotherapy for CTCL and other solid tumors. *Mol Cancer Ther; 1–11. ©2012 AACR.*

Introduction

Cutaneous T-cell lymphoma (CTCL) is the second most common extranodal non–Hodgkin lymphoma in adults, characterized by primary accumulation of clonally derived malignant $CD4^+$ T cells in the skin. There are 13 clinically and histologically distinct types of CTCL, and the majority falls into 3 classes: mycosis fungoides (MF), the most common type of CTCL, accounts for almost 50% of all primary cutaneous lymphomas; primary cutaneous $CD30^+$ lymphoproliferative disorders—more specifically primary cutaneous anaplastic large cell lymphoma (PC-ALCL)—the second most common CTCL, account for circa 30%; and Sézary syndrome, the most aggressive type of CTCL, makes up circa 5% (1, 2). Other forms of CTCL include adult T-cell leukemia/lymphoma (ATLL; 2%–5%) and peripheral T-cell lymphoma (PTCL; 2%). Although CTCL usually has indolent clinical behavior, in advanced stages, it can progress into an aggressive phenotype with poor prognosis and survival (1, 3, 4) with severe immunodeficiency characteristically developing during disease progression (5). Current hypotheses maintain that the malignant T cells drive this evolving immunodeficiency through the constitutive secretion of immunosuppressive cytokines, dysregulated expression of immunoregulatory proteins by the malignant T cells, and loss of TCR repertoire complexity due to competitive replacement of normal T cells by the clonally expanded malignant T cells. In addition, a subset of the malignant T cells may act as T-regulatory cells (Tregs) to suppress antitumor responses in some patients with CTCL (6–8). Current therapies for CTCLs do not prevent new lesions from emerging (9) and durable long-term remissions are rare (10). Therefore, disease-specific and more effective therapeutics that can

Authors' Affiliations: [1]Department of Cancer Immunology and AIDS, Dana-Farber Cancer Institute; [2]Department of Medicine, Harvard Medical School; and [3]Department of Dermatology, Harvard Skin Disease Research Center, Brigham and Women's Hospital, Harvard Medical School, Boston, Massachusetts

Note: Supplementary data for this article are available at Molecular Cancer Therapeutics Online (http://mct.aacrjournals.org/).

Corresponding Authors: Wayne A. Marasco, Dana-Farber Cancer Institute-Harvard Medical School, 450 Brookline Ave., Boston, MA 02215. Phone: 617-632-2153; Fax: 1-617- 632-3889; E-mail: wayne_marasco@dfci.harvard.edu; Thomas S. Kupper, E-mail: tkupper@partners.org; and Quan Zhu, E-mail: quan_zhu@dfci.harvard.edu

doi: 10.1158/1535-7163.MCT-12-0278

decrease toxicity profiles and induce durable responses will greatly benefit patients with CTCL.

Normal skin-homing $CD4^+$ T cells express cutaneous lymphocyte–associated antigen and CC chemokine receptors (CCR) CCR4, CCR6, CCR7, and CCR10 (11–14). Among these, only CCR4 is universally expressed at high levels on the malignant skin-homing T cells, and its surface expression is closely associated with the enhanced skin-homing characteristics of CTCL cells and unfavorable disease outcome (15, 16). Tregs also selectively express high levels of CCR4 compared with other T-cell subsets. The 2 specific ligands for CCR4, chemokines CCL17, and CCL22, produced by tumor cells and cells of the tumor microenvironment, attract $CCR4^+$ Tregs to the tumor, where they suppress host immune responses against tumor and create a favorable environment for cancer cells to grow (17, 18). Thus, the high-level expression of CCR4 on CTCL cells and its preferential expression on Tregs (19) make CCR4 not only a potential ideal therapeutic target for CTCLs, but also for other type of cancers for which $CCR4^+$ Tregs are involved in their immune evasion.

In this study, we characterized and humanized a mouse anti-CCR4 monoclonal antibody, mAb1567, that recognizes both the N-terminal (NT) and the extracellular domains of CCR4. The antibody exhibited potent antitumor effects in a CTCL mouse model and its mechanism(s) of action, including complement-dependent cytotoxicity (CDC), neutrophil,- and NK-mediated antibody-dependent cellular cytotoxicity (ADCC), were elucidated by a number of *in vitro* studies. In addition, mAb1567 could not only inhibit Tregs migration toward CCR4 ligand, CCL22, but also abrogate suppression by Tregs in the T-cell proliferation assay. Finally, after the affinity maturation of humanized mAb1567, the resulting mAb2-3 was further improved in affinity and showed stronger CDC and ADCC activities against $CCR4^+$ tumor cells.

Materials and Methods

Cells

Mac-1 cell line was isolated from a patient with PC-ALCL, one of CTCLs (20), obtained from Dr. Thomas S. Kupper (Brigham and Women's Hospital, Harvard Medical School, Boston, MA) and cultured in 10% FBS RPMI-1640. Luciferase-expressed Mac-1 cells were stably transduced with a luciferase reporter retrovirus and authenticated by detecting luminescence. 293F cell line was purchased from Invitrogen. 293T (CRL-11268) and Cf2Th (CRL-1430) cell lines were purchased from American Type Culture Collection and incubated in 10% FBS Dulbecco's modified Eagle's medium. No additional authentication of these cell lines was conducted by the authors.

Antibodies and flow cytometry analysis

mAb1567 was purchased from R&D systems and the other 1567 variant antibodies were produced as described previously (21). Briefly, scFv-Fcs were constructed by cloning the single-chain variable region (scFv) into pcDNA3.1-Hinge vector in frame with human IgG1 Fc region. IgG1 was generated by cloning heavy-chain variable region (VH) and light-chain variable region (VL) into TCAE5.3 vector (22). Antibodies were produced in 293T or 293F cells and purified by proteinA-Sepharose (Amersham) affinity chromatography. For staining, Mac-1 was stained with anti-CCR4 antibodies, detected by fluorescein isothiocynate (FITC)-conjugated goat–anti-human IgG or anti-mouse IgG antibodies (Sigma), and analyzed with FACSCalibur and CellQuest software.

Chemotaxis

Mac-1 cells (1×10^6 cells/well) were placed in Transwell migration wells (Corning) with or without mAb1567 for 3 hours at 37°C. Migrated cells harvested from the bottom chamber containing 50 ng/mL human CCL17 or CCL22 (R&D Systems) were enumerated by fluorescence-activated cell sorting (FACS) analysis. Human $CD4^+$ T cells were isolated by $CD4^+$ T-cell isolation kit (Miltenyi Biotech) and placed in Transwell migration assays with c1567IgG. Migrated cells ($CD4^+CD25^{high}$) were enumerated as above in response to 100 ng/mL CCL22. Percentages of migrated cells were calculated by dividing the number of transmigrated Mac-1 or $CD4^+CD25^{high}$ cells by the number of input cells.

Antibody-dependent cell cytotoxicity assay

For lactate dehydrogenase (LDH) release assay, SCID/Beige mouse neutrophils, human peripheral blood mononucleated cells (PBMC), or human NK cells and neutrophils were used as effector cells and Mac-1, Cf2Th-CCR4, or Cf2Th were used as target cells. Target cells (1×10^4 cells/well) were plated into 96-well plates and antibodies were added. After 1 hour, effector cells were added at an appropriate effector/target (E/T) ratio and incubated (PBMCs, NK, and neutrophils for 4, 16, and 6 hours, respectively). The supernatants were recovered by centrifugation at $300 \times g$ and measured using nonradioactive cytotoxicity assay kits (Promega) at 490 nm. For ^{51}Cr release assay, 1×10^6 Mac-1 cells were labeled with 100 μCi (3.7 MBq) of $Na^{51}Cr$ (Amersham International), washed, and used as targets. ^{51}Cr-labeled target cells (5,000 cells/well) were seeded into 96-well plates and the release of ^{51}Cr into supernatants was determined. The cytotoxicity was calculated by the following formula:

$$\% \text{ Cytotoxicity} = 100 \times (E - S_E - S_T)/(M - S_T)$$

where E is released LDH from E/T culture with antibody; S_E, spontaneous released LDH from effectors; S_T, spontaneous released LDH from targets; and M, the maximum released LDH from lysed targets.

Complement-dependent cytotoxicity assay

5×10^4 Mac-1 cells per well, resuspended with medium containing rabbit serum (Cedarlane Laboratories) or mouse serum (IMS-COMPL; Innovative Research), were plated in 96-well plates with anti-CCR4 antibodies. After

4-hour incubation, the supernatants were recovered and detected by LDH release assay, calculating as: % Cytotoxicity $= 100 \times (E - S_E - S_T)/(M - S_T)$.

Regulatory T-cell suppression assay

$CD4^+CD25^{high}$ and $CD4^+CD25^-$ T cells were sorted by Beckman CoulterMoFlo sorter using mouse-anti-human CD4-PE-Cy5 (RPA-T4) and antihuman CD25-PE (M-A251) antibodies (BD Pharmigen). $CD4^+CD25^-$ Teffs (2,500) were cultured with or without $CD4^+CD25^{high}$ Tregs (1,250) in 96-well plates with 25,000 irradiated (3,000 rad) CD3-depleted PBMCs. Cells were stimulated with 0.05 μg/mL plate-bound anti-CD3 (UCHT1) and 1 μg/mL soluble anti-CD28 (CD28.2) antibodies (BD Pharmigen). Anti-CCR4 antibodies were included in the appropriate cultures. The cultures were pulsed on day 5 after culture initiation with 1 μCi ^{3}H-labeled thymidine/well (Perkin Elmer). Proliferation of cultures was measured in terms of incorporation of ^{3}H-thymidine by reading counts in a scintillation counter (Perkin Elmer).

$CCR4^+$ CTCL tumor-bearing mouse model

2×10^6 luciferase-Mac-1 or 1×10^7 Mac-1 cells were injected subcutaneously into the dorsolateral flank in 6-week SCID/Beige mice (Charles River). After 24 hours of injection, mice were randomly assigned into different groups and treated with 3 mg/kg of mAb1567 and mouse IgG2b (twice a week for 3 weeks) or 5 mg/kg of control-scFv-Fc, c1567-scFv-Fc, and h1567-scFv-Fc (twice a week for 4 weeks) by intraperitoneal injection. Body weight and tumor size were measured using digital caliper and Xenogen imaging. Tumor volumes were calculated as length $\times$ $(\text{width})^2 \times 0.52$. Animal care was carried out in accordance with the guidelines of Animal Care and Use Committee of Dana-Farber Cancer Institute (Boston, MA).

Statistical analyses

Data were analyzed using 2-sided unpaired Student *t* test. "$*$," "$**$," and "$***$" indicate $P < 0.05$, 0.01, and 0.001, respectively. All values and bars are represented as mean $\pm$ SD.

Results

Characterization of a mouse anti-CCR4 mAb and mAb1567, *in vitro* and *in vivo*

CCR4 has 4 regions exposed at the cell surface: the NT (~30–50 aa) and 3 extracellular domains loops (ECL, each of ~10–30 aa), which are important for ligand binding, intracellular signaling, and other biologic functions. In this study, 2 commercially available murine anti-CCR4 mAbs, mAb1567 (R&D systems), and 1G1 (BD Pharmingen), both generated by immunizing mouse with full-length human CCR4 (hCCR4)-expressing cells (13, 23), were initially selected for evaluation. Both mAb1567 and 1G1 showed specific binding activity in FACS analysis to hCCR4-expressing Cf2Th-CCR4 cells but not to the parental Cf2Th cells. In comparison, mAb1567 had relatively higher affinity than 1G1 under the same antibody concentrations tested (data not shown). Therefore, we selected only mAb1567 for further characterization.

Binding of mAb1567 was further tested using the $CCR4^+$ Mac-1 cells by FACS analysis and the half maximal effective binding concentration (EC_{50}) is about 0.45 nmol/L (Fig. 1A). Chemotaxis inhibition assay showed that mAb1567 effectively inhibited chemotaxis of Mac-1 cells in a dose-dependent manner toward both CCR4 ligands, CCL17 and CCL22 (Fig. 1B). We next examined the epitope recognized by mAb1567, in particular, whether it recognizes solely the NT or a nonlinear conformational-dependent epitope comprising of both NT and ECL, by using hCCR4 and hCCR8 NT swapping chimeras that either contained CCR8-NT/CCR4-ECLs (Chi#1) or CCR4-NT/CCR8-ECLs (Chi#2; ref. 24). As shown in Supplementary Fig. S1A, all constructs encoding wild-type or chimeras CCR4 and CCR8 expressed similar levels on the cell surface as validated by antibody staining against the HA tag. mAb1567 specifically recognized cell surface full-length hCCR4 but not hCCR8. It bound to Chi#1 and Chi#2 in a similar level as WT CCR4 indicating that the epitope of mAb1567 is not solely a linear epitope on NT of CCR4, rather both ECLs and NT contribute to the binding of mAb1567 with CCR4. However, the CCR4-Nt alone is also sufficient for some degree of mAb1567 binding to CCR4-Nt-Fc as determined in ELISA studies to plate-bound mAb1567 (Supplementary Fig. S1B–S1D). Moreover, mAb1567 showed high specificity for CCR4 rather than CCR5, the most similar CCR molecule to CCR4 (Supplementary Fig. S1E).

We then tested the antitumor effect of mAb1567 *in vivo* in a CTCL model using immunodeficient SCID/Beige mice that lack T and B cells and have defective NK function. SCID/Beige mice implanted with Mac-1 cells can efficiently form subcutaneous tumors (25). As shown in Fig. 1C, the tumor size in the mAb1567-treated group was 3- to 4-fold smaller than seen in the control group. None of the mice showed mAb1567 treatment–related toxicity.

mAb1567 mediates against Mac-1 cells both CDC in the presence of mouse and rabbit complement and neutrophil ADCC

To further understand the mechanism underlying the antitumor effect of mAb1567 seen in the SCID/Beige mice, we tested whether mAb1567 can mediate CDC and/or neutrophil-mediated ADCC effects against $CCR4^+$ tumor cells *in vitro*. mAb1567 induced a significant lysis of Mac-1 cells in a dose-dependent manner in the presence of mouse complement as compared with the mouse IgG2b isotype control antibody (Fig. 2A). Rabbit complement was also tested and mAb1567 mediated a much more potent CDC activity and reached 80% of the target cell lysis (Fig. 2B). Next, neutrophils isolated from the SCID/Beige mice were tested in an *in vitro* ADCC assay. As shown in Fig. 2C, mAb1567 specifically mediated approximately 20% lysis via mouse neutrophils as compared

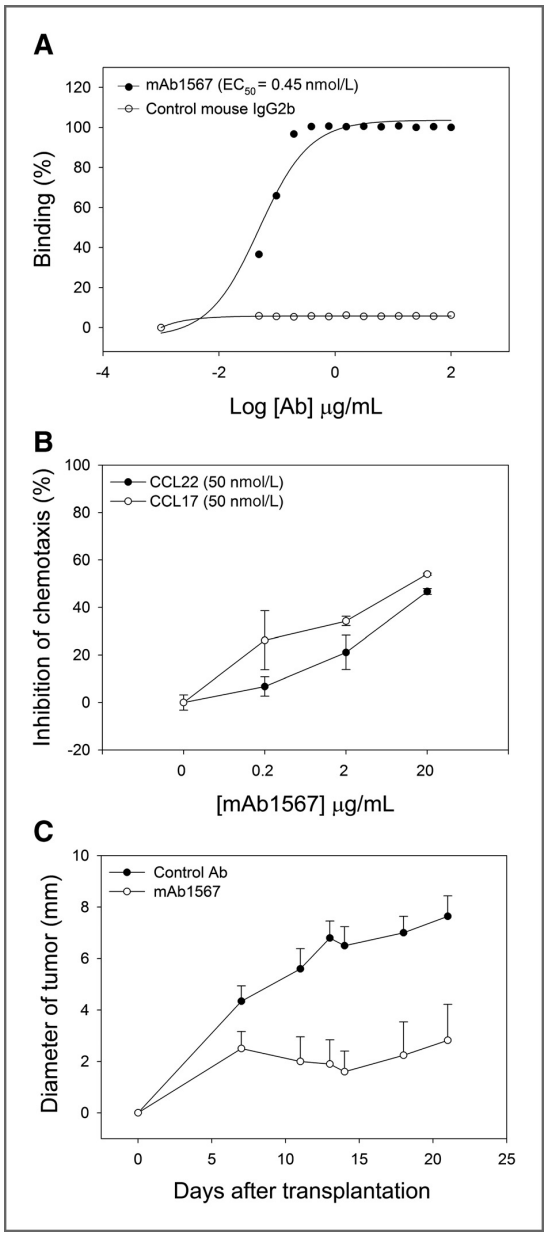

Figure 1. Overexpression of functional CCR4 on cutaneous T-cell lymphoma and mouse anti-CCR4 mAb1567 inhibits tumor formation. A, dose-dependent binding curve of mAb1567 to CCR4$^+$ Mac-1 cells by FACS analysis. The EC_{50} was generated using SigmaPlot software. B, mAb1567 effectively inhibited chemotaxis of Mac-1 cells to CCR4 ligands, CCRL22 and CCL17. C, the antitumor effect of mAb1567 in SCID/Beige mice–bearing Mac-1 xenografts.

with control at E/T (neutrophils/Mac-1) ratio of 80:1. These results show that mAb1567 can directly mediate not only CDC but also mouse neutrophil-induced ADCC activities.

Cloning, expression, and activity of chimeric mAb1567

To humanize mAb1567 for further preclinical studies, the cDNAs encoding the *VH* and *VL* genes from the hybridoma cell line were individually recovered by

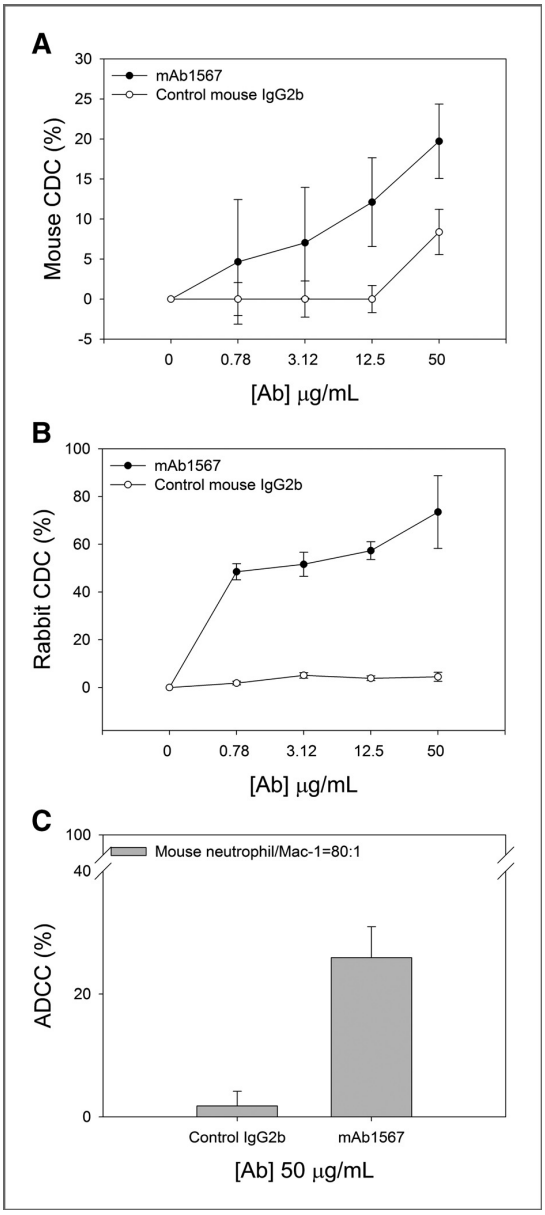

Figure 2. mAb1567 mediates against Mac-1 cells both CDC and neutrophil-ADCC. A, mAb1567-mediated CDC activity *via* mouse complement. Figure shown is one experiment that is representative of at least 3 independent experiments. B, mAb1567-mediated CDC activity with rabbit complement. C, neutrophils from SCID-Beige mice–mediated mAb1567-dependent ADCC.

RT-PCR using primers specific for mouse antibody variable genes. The VH and VL of mAb1567 belong to mouse V_H1 (IGHV1S56*01) and V_K8 (IGKV8-27*01) families and were rearranged with the J_H1 (IGHJ1*01) and J_K2 (IGKJ2*01) segments, respectively. The cloned and rearranged *VH* and *VL* genes were then assembled as a single-chain antibody variable region fragment (scFv) using a $(G_4S)_3$ linker. Binding of the recombinant mAb1567 to CCR4 was verified in both scFv-Fc IgG1 minibody (c1567-scFv-Fc; Fig. 3A) and full-length chimeric IgG1 form (c1567-IgG; data not shown).

As NK cell–mediated ADCC is one of the most important mechanisms of action for immunotherapy with human IgG1 Abs, we further tested whether recombinant mAb1567 can mediate ADCC via NK cells. Chimeric 1567 in both scFv-Fc or IgG1 forms were highly effective in killing Mac-1 cells in an *in vitro* ADCC assay using human PBMCs (Fig. 3B) or purified NK ($CD56^+CD16^+$) cells (Fig. 3C) from healthy donors as effector cells at different E/T ratios.

Humanization of mAb1567 and related biologic studies

Next, the structure-guided complementarity-determining region (CDR) grafting approach was used to humanize mAb1567. Homology 3-dimensional modeling of the VH and VL chains of mAb1567 using Web Antibody Modeling program (26) was generated to known antibody structures in the PDB database. For selecting the human acceptor framework template for CDR-grafting, the VH and VL amino acid sequences of mAb1567 were separately compared with human Ab sequences in the IGBLAST database to identify the most similar human Ab and Ig germline VH and VL sequences (Fig 3D). The human VH (McAb Ctm01, PDB:1ae6H) and VL (GenBank #ABG38372) share 82% and 84% amino acid sequence homology to the VH and VL of mAb1567, respectively; the best matched human Ig germline V sequences are IGHV1-3*01 (67% homology to mAb1567-VH) and IGKV4-1*01 (83% homology to mAb1567-VL). The framework residues of mAb1567 were manually changed to the selected human framework residues to generate the humanized mAb1567 (h1567). GROMOS force field energy minimization parameter was then applied to homology model h1567 using DeepView program (27). Examination of this energy minimized homology model of h1567 was carried out to ensure that no residues had distorted geometry or steric clashes with other residues.

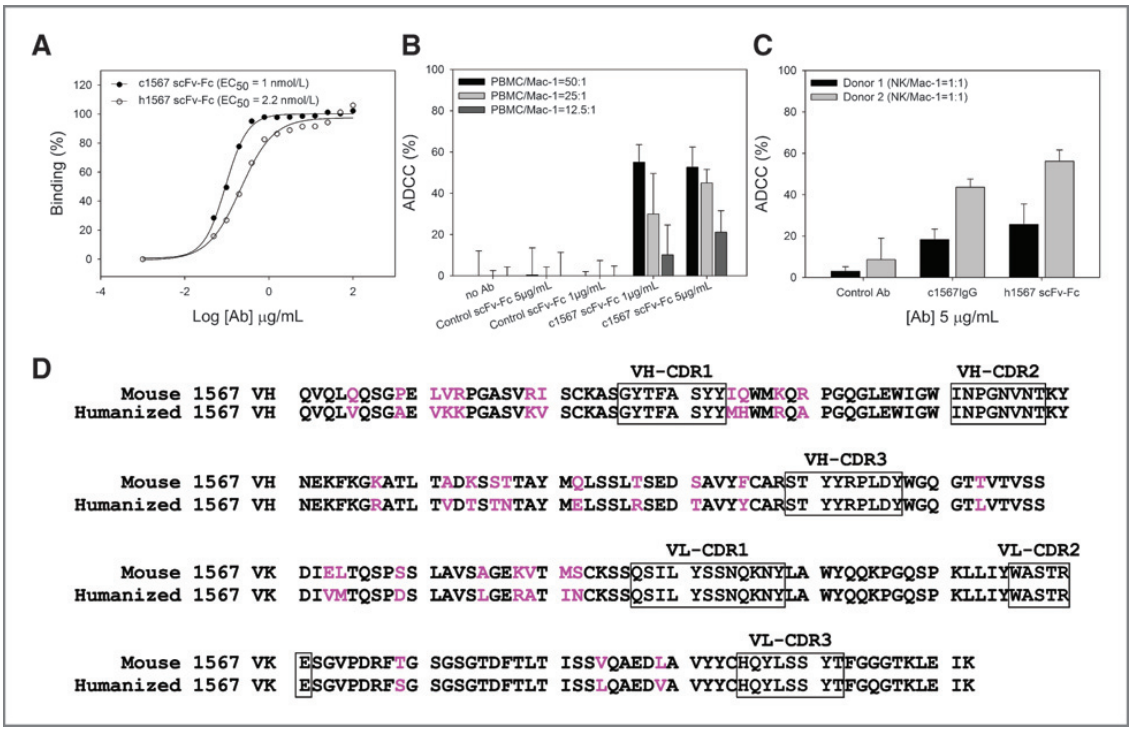

Figure 3. Humanization of mAb1567 and function analysis. A, comparative binding analysis of c1567 and h1567 scFv-Fcs. B, C, ADCC activity mediated by c1567 scFv-Fc. Either PBMCs (B) or NK cells (C) from healthy donors were used as effector cells. Target cell lysis was measured either by Cr^{51} (B) or LDH release (C). Data were calculated from triplicate wells of one experiment and are representative of 3 independent experiments. D, amino acid sequence alignment of the rearranged mouse and humanized variable heavy (VH) and variable light (VK) κ domains. Residues in magenta indicate framework residues that were changed for humanization.

The h1567 sequence shown in Fig. 3D has 21 and 11 amino acid differences in the framework regions compared with the mouse VH and VL, respectively. The humanized *VH* and *VL* gene were *de novo* synthesized and codon-optimized for mammalian cell expression. The binding affinity of h1567 and c1567 scFv-Fcs to CCR4 was then compared by FACS with Mac-1 cells. The h1567 had approximately 2-fold decrease in binding as compared with c1567 but both are in the nanomolar range, with EC_{50} of 2.2 and 1 nmol/L, respectively (Fig. 3A). The humanized h1567 scFv-Fc maintained potent NK-mediated ADCC killing of Mac-1 cells compared with c1567 (Fig 3C).

To test the *in vivo* antitumor effect of h1567, the luciferase-expressing Mac-1 cells were subcutaneously implanted into the dorsolateral flank of SCID/Beige mice, and mice were intraperitoneally treated with 5 mg/kg of control-scFv-Fc, c1567-scFv-Fc, h1567-scFv-Fc, or equivalent volumes of saline. Tumor growth in mice was monitored for luciferase intensity by IVIS imaging. All mice were sacrificed on day 28 and tumors were excised for photographing and measuring tumor weight. As shown in Fig. 4, tumors were significantly reduced in size at day 21 in c1567- and h1567-treated groups but not in control-scFv-Fc or PBS-treated groups as measured by IVIS imaging (Fig. 4A, top, and C), size of the excised tumors (Fig. 4A, bottom), tumor volume (Fig. 4B), and tumor weight (Fig. 4D).

ADCC and CDC activities of higher affinity h1567 variants

Although the h1567 exhibited similar biologic activity as its murine counterpart in both *in vitro* and *in vivo*, the relative apparent binding affinity of h1567 is 2-fold lower than c1567 (Fig. 3A). To further affinity mature the h1567, we conducted VL-chain shuffling and alanine scanning to identify key residues in CDRs, followed by selection and screening of phage display library constructed by random mutagenesis of key residues in the CDRs (see Supplementary Method and SupplementaryFig. S2 for details).

The 2 affinity-improved h1567 variants, mAbs 1-44 and 2-3, that showed higher binding affinity to Mac-1 cells than parental h1567 with EC_{50} of 1.47 and 1.39 nmol/L, respectively (Supplementary Fig. S2F) were further evaluated for their capacity to mediate ADCC activity using human NK cells. The result showed that improvement in ADCC activity of the h1567 variants is correlated with their binding affinity, 2-3-scFv-Fc exhibited the best human NK-mediated ADCC activity for both Mac-1 cells (Fig. 5A) and Cf2Th-CCR4 cells but not to negative control Cf2Th (Supplementary Fig. S3). Moreover, because parental mAb1567 could induce mouse neutrophil-mediated ADCC, h1567 and 2-3 were tested for human neutrophil-mediated ADCC assay and mAb2-3 showed enhanced cytotoxic activity (Fig. 5B) compared with h1567. Furthermore, slightly improved CDC activity against Mac-1 cells was also observed for both 1-44 and 2-3 variants, but more for the 2-3-scFv-Fc (Supplementary Fig. S4).

Fc engineering was also conducted on mutant Abs 1-44 and 2-3 to further enhance ADCC activity by mutating 3 residues (S239D, A330L, and I332E) in CH2 domain, which have been shown to increase ADCC effect of human IgG1 antibody (28). As shown in Fig. 5C, ADCC-mediated by 1–44- and 2-3-scFv-mFcs was significantly enhanced as compared with their WT Fc counterparts or the WT h1567. However, as the A330L mutation in the Fc domain can ablate CDC function (29), we also tested and confirmed that CDC activity for the scFv-mFcs forms of 1-44 and 2-3 scFv-mFcs was completely abolished (Fig. 5D). Taken together, the affinity optimized variants of humanized 1567, in particular the 2-3 variant, showed improved ADCC and CDC effector functions, and NK cell–mediated ADCC activity can be further enhanced through Fc engineering.

mAb1567 inhibits Tregs chemotaxis and partially abrogates Tregs' suppressive activity *in vitro*

Finally, as the majority (94%) of freshly isolated $CD4^+CD25^{high}$ Tregs from peripheral blood express high level of surface CCR4 (30) and they have been reported to migrate to tumors secreting CCL22 (31), we investigated whether Ab1567 could have an antitumor role by modulating the chemotactic recruitment and suppressive activity of human $CD4^+$ Tregs. First, we confirmed that $CD4^+CD25^{high}$ Tregs migrated toward CCL22 much more effectively than $CD4^+CD25^-$ T cells (Fig. 6A). Next, using peripheral blood $CD4^+$ T cells in combination with examining the Treg phenotype of the migrated cells, we confirmed that c1567 completely inhibited the migration of $CD4^+CD25^{high}$ Tregs in a transwell chemotaxis assay at concentrations greater than 2 μg/mL (Fig. 6B).

In addition, as we are unaware of any published data on the role of CCR4 in Treg function, we also examined whether 1567 engagement of CCR4 could result in modulation of Treg suppression activity in an *in vitro* Treg suppression assay. As shown in Fig. 6C, the proliferation of $CD4^+$ T-effector cells (Teffs alone, lane 1) was inhibited by highly purified $CD4^+CD25^{high}$ Tregs (1:2 ratio) by 78% (lane 7), which is our typical Treg suppression effect on Teffs (32). Surprisingly, in the presence of c1567IgG or h1567scFv-Fc, the proliferation of Teff was stimulated to 183% and 207%, respectively (lanes 3 and 5), but there was no stimulatory effect on Treg (lanes 4 and 6). In the Treg/Teff coculture (1:2 ratio), the proliferation of Teff was inhibited directly (lane 7) and there was no reversal of this inhibition by control mAb (lane 8). Moreover, T-cell proliferation was restored with a net positive response to 258% and 221% (lanes 9 and 10) in the presence of c1567IgG or h156scFv-Fc, respectively.

The increase in $CD4^+CD25^-$ T-cell proliferation in the presence of anti-CCR4 antibodies was further observed by flow cytometry. We detected $CD4^+CD25^-$ T-cell proliferation on the basis of CFSE fluorescence intensity of labeled $CD4^+CD25^-$ T cells in the Treg/Teff coculture. The analysis revealed that over the 7-day study, $CD4^+CD25^-$ T-cell proliferation responded to stimulation of anti-CCR4

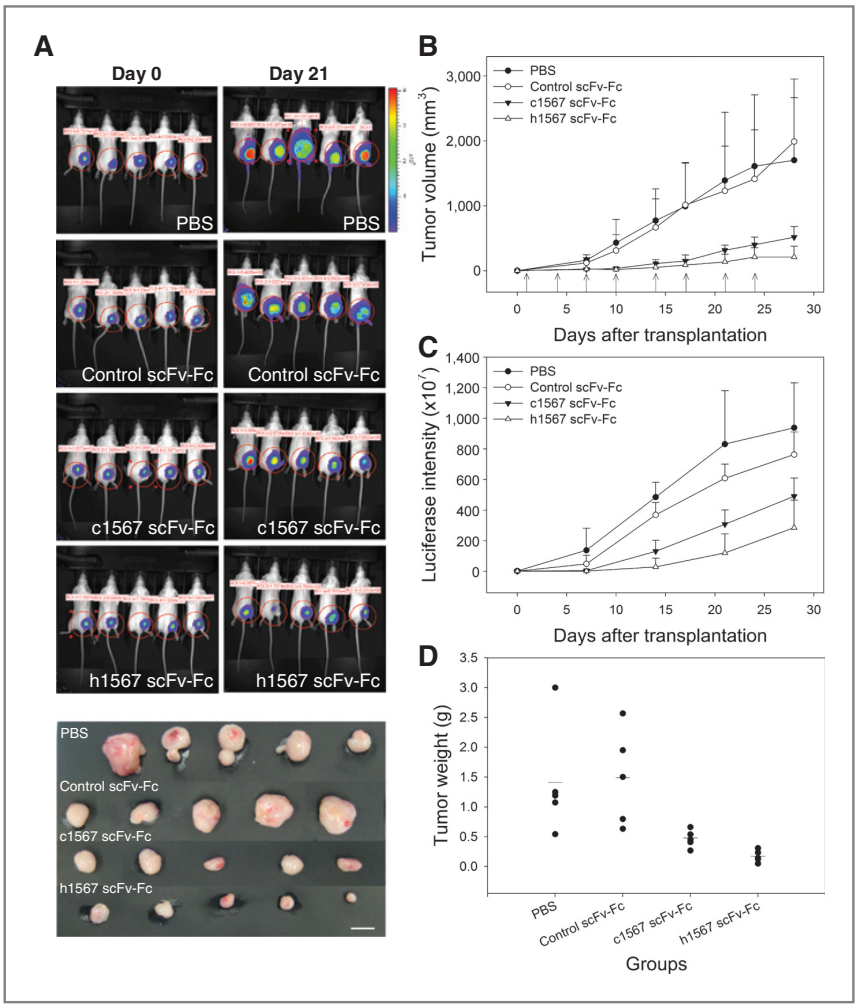

Figure 4. Humanized 1567 in tumor treatment. A, mice-bearing Mac-1 tumors were imaged using an IVIS imaging system. Luciferase signal (top) and tumor size (bottom) in mice treated with anti-CCR4 antibodies. Color scale: blue, luminescent signal intensity; red, least intense signal; most intense signal. Bar scale, 1 cm. B, tumor sizes, image intensity (C), and tumor weight (D) were measured.

antibodies in a time-dependent manner and was approximately 50% higher than with control antibody–treated cells that showed no proliferation (Supplementary Fig. S5). Importantly, Treg-mediated suppression of Teff proliferation occurred even in the presence of anti-CD3/CD28 costimulation but could be reversed in the presence of anti-CCR4 antibody resulting in an increased proliferative capacity of $CD4^+CD25^-$ T cells.

Discussion

In this study, we humanized a mouse anti-CCR4 antibody, mAb1567, which recognizes both the NT and the ECLs of CCR4 with high affinity and inhibits migration of $CCR4^+$ tumor cells toward its 2 ligands, CCL22 and CCL17. The antibody exhibited potent antitumor effect in a CTCL mouse model with the mechanisms of CDC and neutrophil-mediated ADCC likely involved (Figs. 1 and 2). The chimeric or humanized mAb1567 also showed potent CDC and human NK cell–mediated ADCC activity *in vitro* and therapeutic effects *in vivo* (Figs. 3 and 4). In addition, this antibody effectively inhibited the chemotaxis of $CD4^+CD25^{high}$ Tregs to CCL22. Interestingly, it also stimulated $CD4^+CD25^-$ cell proliferation and inhibited Tregs' immune-suppressive activity (Fig. 6 and Supplementary Fig. S5). The affinity of h1567 was further improved by employing a targeted mutagenesis strategy in combination with phage-display library selection and the affinity optimized h1567 variant mAb2-3 showed better CDC and ADCC activities against $CCR4^+$ tumor cells *in vitro* (Fig. 5). These studies support that the affinity selected mAb2-3 may provide a novel immunotherapy option not only to directly kill the $CCR4^+$ tumor cells, but also may have a role in other cancers by suppressing Treg trafficking and overcoming the suppressive effect of $CCR4^+$ Tregs to enhance host antitumor immune responses.

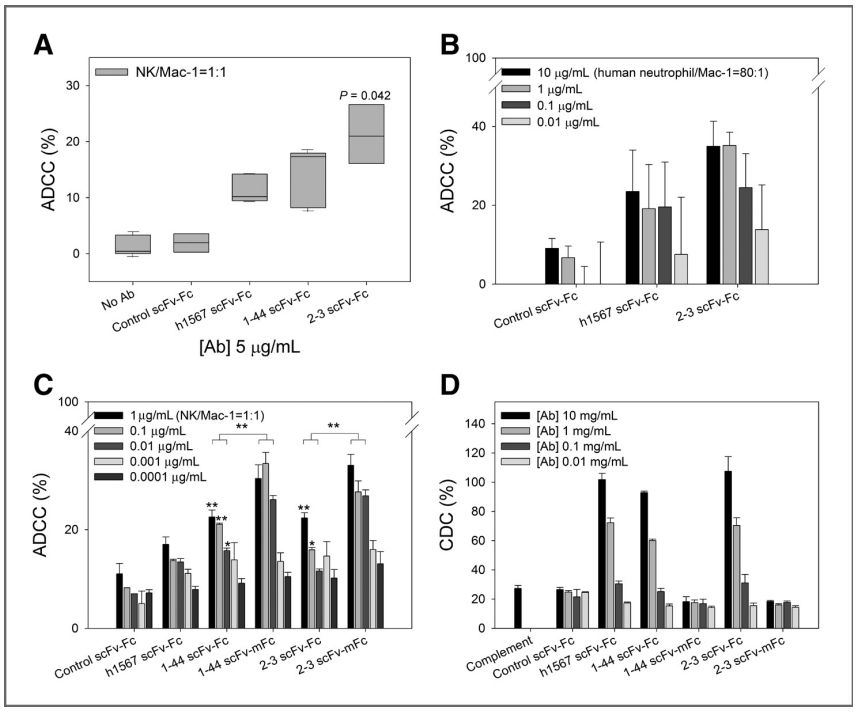

Figure 5. Humanized 1567 variants with improved binding affinity, ADCC, and CDC activity. A, H1567 and its variants 1-44 and 2-3 were tested in the ADCC activity. Data shown in the box and whiskers graph represent 3 independent experiments and each was carried out with NK cells from a different healthy donor; the box extends from lowest percentile to the highest percentile, with a line at the median. The whiskers above and below the box indicate the 95th and 5th percentiles. B, ADCC activities on Mac-1 with human neutrophils. C, ADCC activities on Mac-1 with human NK cells. D, CDC of wild-type Fc antibodies (scFv-Fcs) and mutant Fc antibodies (scFv-mFcs) against Mac-1.

A number of studies have been reported on a humanized anti-CCR4 antibody, KM-0761 (33, 34). These studies have not only showed KM-0761's effect in CTCL tumor animal models and its mechanism of action, but also convincing support that CCR4 is an important antibody-based immunotherapy target for relapsed $CCR4^+$ ATL or PTCL (35, 36). The KM-0761 antibody was originally raised in mouse by immunizing with the CCR4's $NT_{(12–29)}$ peptide (34, 37), it works in killing tumor cells by ADCC mainly through NK and/or macrophages (33, 38, 39), and augmentation of FcγR engagement and ADCC killing is achieved by defucosylation (34). In contrast, mAb1567 was generated with full-length CCR4, it recognizes an epitope comprising of both NT and ECLs of CCR4, and ADCC-enhanced killing is achieved through both affinity maturation and Fc engineering (29). In addition, mAb1567 showed both CDC and ADCC activity. The disparity in CDC activities between these 2 IgG1 antibodies is likely due to different recognition of the CCR4 epitope(s). CDC is often dependent on the distance between the plasma membrane and the constant region of the sensitizing antibody that mediates effector functions (40). It is possible that the CDC activity mediated by mAb1567 is related to the position and orientation of the recognized epitope, when bound, the mAb1567 can position its Fc region more proximal to the membrane to recruit complement efficiently. Another possibility is that binding to the different epitope may promote more efficient cross-linking of CCR4, and thus, increasing the binding avidity (41).

Antitumor effect mediated by cancer cell–directed antibodies can generally be attributed to ADCC, CDC, or direct antiproliferation. We found that mAb1567 did not show any inhibition of cell proliferation (data not shown). Effector cells that can mediate ADCC are NK cells, neutrophils, and monocytes/macrophages. The SCID/Biege mice used in our *in vivo* studies not only lack T- and B-lymphocytes but are also NK cell defective. Thus, we surmised that the antitumor activity of mAb1567 seen in SCID/Beige mice might be due to effector cells other than NK cell–mediated ADCC and/or to CDC. *In vitro* CDC experiments indeed showed that mAb1567 had CDC activity as compared with control Ab, although the level of lysis target Mac-1 cells was low, upto approxiamtely 20%. Most mouse strains (including the mouse stains tested here) have exceptionally low complement activity, much lower than that of humans or other animals, including rabbits, guinea pigs, and hamsters (42). CDC assay with rabbit complement indeed showed dramatically improved lysis of target cells by mAb1567 (Fig. 2B) upto approximately 80%. Furthermore, mAb1567 could mediate ADCC activity (approximately 25%) via neutrophils isolated from SCID/Beige mice. Because of limited number of neutrophils available, only a single dose of mAb1567 and isotype control mAb at 50 μg/mL was tested (Fig. 2C). These results suggest that the antitumor activity of mAb1567 in the mouse model is likely due to a combination of both CDC and through neutrophil-mediated ADCC, although it remains to be tested if mouse monocytes/macrophages may also play a role.

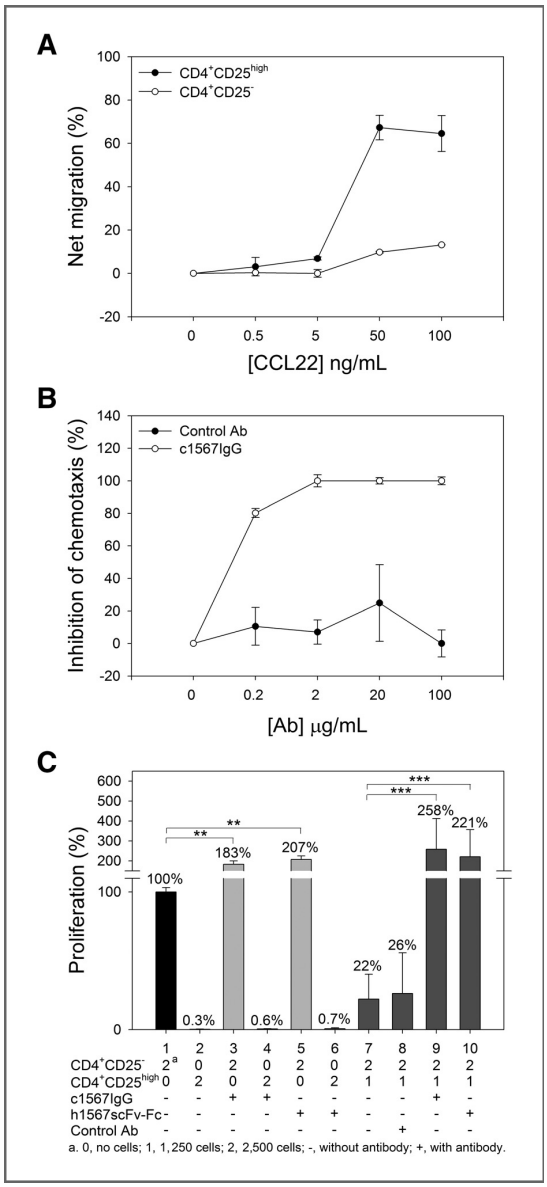

Figure 6. Anti-CCR4 antibody abrogates suppression by Tregs. A, $CD4^+CD25^{high}$ T cells showed demonstrable chemotactic responses toward CCL22. B, chimeric mAb1567 effectively inhibited chemotaxis of Tregs to CCL22. C, the effect of anti-CCR4 antibodies on proliferation of Teffs and the abrogation of the suppressive function of Tregs. The percent proliferation was normalized to $CD4^+CD25^-$ Teffs without antibody treatment.

Many therapies for cancer are accompanied by adverse side effects and dose-dependent toxicities. The development of more effective cancer immunotherapy with better discrimination between tumor cells and normal cells is the most important goal of current anticancer research. CCR4 is universally expressed at high levels among most CTCL cells; however, a subset of normal T cells also can express CCR4. It was reported that the CCR4 is selectively expressed on T-helper 2 (T_H2) cells, but not T_H1 cells, which are the precursors of memory T cells (43). Of particular importance to the *in vivo* expression of CCR4 on T_H2 cells would be a concern of bystander cytotoxicity in response to anti-CCR4 antibody treatment. However, potential bystander effects can be managed as shown in the recent clinical trial reports on the anti-CCR4 mAb, KW-0761, for treatment of ATLL and PTCL, where good clinical activity was seen without serious side effects (35, 36). This may be due, at least in part, to the CCR4-expressing CTCL patient cells showing a significantly 4-fold higher expression level than T cells from healthy donors (44). This high CCR4 expression in CTCL patients may result in most anti-CCR4 antibody binding to tumor T cells but not normal T cells. We are also aware of reports that CCR4 is expressed on platelets (45, 46) but again in the KW-0761 clinical trial (35), grade 3 or 4 thrombocytopenia was only seen in 5 of 28 patients (18%) and not associated with bleeding.

CCR4 is also highly expressed on the majority (94%) of $CD4^+CD25^{high}FoxP3^+$ Tregs (30) that are considered the most potent inhibitors of antitumor immunity and the greatest barrier to successful immunotherapy (31, 47). CCR4 also plays an important role in Treg recruitment to the site of action. In some solid tumors including breast cancer (17, 48), ovarian cancer (18), and oral squamous cell carcinoma (49), increased numbers of recruited Tregs that are chemoattracted through the CCR4–CCL22 axis likely play a significant role in the suppression of host antitumor immunity. This trafficking pattern makes CCR4 an even more attractive therapeutic target for a broader range of tumors. mAb1567 was tested for inhibition of Treg migration and showed complete inhibition of chemotaxis of $CD4^+CD25^{high}$ Tregs (Fig. 6A). Interestingly, it appeared that mAb1567 can also abrogate the immune suppressive function of $CD4^+CD25^{high}$ Tregs while stimulating the proliferation of $CD4^+CD25^-$ Teffs (Fig. 6C and Supplementary Fig. S5). It has been proposed that Tregs exert their function by multiple suppressive mechanisms including cell–cell contact, including competitive consumption of IL-2, production of the immunosuppressive cytokines IL-10 and TGF-β, cytolysis, metabolic disruption, and modulation of the function of antigen-presenting cells (5, 47). However, CCR4 is not known to play a role in $CD4^+CD25^-$ cell proliferation and although a previous study described that $CCR4^{-/-}$ Tregs are defective in suppressive activity in a model of colitis, this was due to their lack of chemotactic recruitment to the mesenteric lymph nodes because their *in vitro* suppressive function was intact (50). It will be important to conduct additional studies to further confirm these findings and elucidate the mechanism(s) by which anti-CCR4 mAb1567 could act through CCR4 on these cells to exercise different functions—proliferative effect on $CD4^+CD25^-$ Teffs and partial to complete abrogation of Tregs' suppression.

In summary, we have humanized and affinity matured murine anti-CCR4 antibody 1567 and showed its *in vitro* and *in vivo* antitumor activity against CTCL cells. The mechanisms of tumor cell killing by mAb1567 seem to be multiple including CDC as well as neutrophil- and NK cell–mediated ADCC. The affinity-matured mAb2-3 promoted more potent CTCL lysis by augmentation of both NK cell–mediated ADCC and CDC activities. Remarkably, the activity of mAb1567 also extended to the normal T-cell compartment with demonstrable proliferative effect on $CD4^+CD25^-$ Teffs and abrogation of Treg suppression. These findings support further evaluation of our anti-CCR4 antibody as an immunotherapy for CTCL and other cancers where augmentation of Teff functions against the tumor cells are likely to have a therapeutic benefit.

Disclosure of Potential Conflicts of Interest

No potential conflicts of interest were disclosed.

Authors' Contributions

Conception and design: J. Sui, M. Bai, R. C. Fuhlbrigge, Q. Zhu, T. S. Kupper, W. A. Marasco

Development of methodology: D.-K. Chang, J. Sui, S. Geng, A. Muvaffak, M. Bai, R. C. Fuhlbrigge, A. S. Lo, Q. Zhu, W. A. Marasco

Acquisition of data (provided animals, acquired and managed patients, provided facilities, etc.): S. Geng, M. Bai, A. Yammanuru, L. Hubbard, J. Sheehan, J. J. Campbell, Q. Zhu, T. S. Kupper

Analysis and interpretation of data (e.g., statistical analysis, biostatistics, computational analysis): D.-K. Chang, J. Sui, S. Geng, M. Bai, A. Yammanuru, Q. Zhu, T. S. Kupper, W. A. Marasco

Writing, review, and/or revision of the manuscript: D.-K. Chang, J. Sui, R. C. Fuhlbrigge, J. Sheehan, Q. Zhu, T. S. Kupper, W. A. Marasco

Administrative, technical, or material support (i.e., reporting or organizing data, constructing databases): D.-K. Chang, J. Sheehan

Study supervision: J. Sui, Q. Zhu, W. A. Marasco

Acknowledgments

The authors thank Maryam Ali, Hong Tao, and Erin M. McConocha for technical support, and National Foundation of Cancer Research (CFCR) for contribution of equipment used in this study.

Grant Support

This work was funded by Skin Cancer Score project 2P50CA093683 to T. S. Kupper, J. Campbell, and W. A. Marasco and NIH AI058804 to Q. Zhu.

The costs of publication of this article were defrayed in part by the payment of page charges. This article must therefore be hereby marked *advertisement* in accordance with 18 U.S.C. Section 1734 solely to indicate this fact.

Received March 19, 2012; revised July 30, 2012; accepted July 30, 2012; published OnlineFirst xx xx, xxxx.

References

1. Willemze R, Jaffe ES, Burg G, Cerroni L, Berti E, Swerdlow SH, et al. WHO-EORTC classification for cutaneous lymphomas. Blood 2005;105:3768–85.
2. Clark RA, Watanabe R, Teague JE, Schlapbach C, Tawa MC, Adams N, et al. Skin effector memory T-cells do not recirculate and provide immune protection in alemtuzumab-treated CTCL patients. Sci Transl Med 2012;4:117ra7.
3. Kim YH, Liu HL, Mraz-Gernhard S, Varghese A, Hoppe RT. Long-term outcome of 525 patients with mycosis fungoides and Sezary syndrome: clinical prognostic factors and risk for disease progression. Arch Dermatol 2003;139:857–66.
4. Kadin ME, Carpenter C. Systemic and primary cutaneous anaplastic large cell lymphomas. Semin Hematol 2003;40:244–56.
5. Krejsgaard T, Odum N, Geisler C, Wasik MA, Woetmann A. Regulatory T-cells and immunodeficiency in mycosis fungoides and Sezary syndrome. Leukemia 2011;26:424–32.
6. Zhang Q, Nowak I, Vonderheid EC, Rook AH, Kadin ME, Nowell PC, et al. Activation of Jak/STAT proteins involved in signal transduction pathway mediated by receptor for interleukin 2 in malignant T lymphocytes derived from cutaneous anaplastic large T-cell lymphoma and Sezary syndrome. Proc Natl Acad Sci U S A 1996;93:9148–53.
7. Kasprzycka M, Zhang Q, Witkiewicz A, Marzec M, Potoczek M, Liu X, et al. Gamma c-signaling cytokines induce a regulatory T-cell phenotype in malignant CD4+ T lymphocytes. J Immunol 2008;181:2506–12.
8. Yawalkar N, Ferenczi K, Jones DA, Yamanaka K, Suh KY, Sadat S, et al. Profound loss of T-cell receptor repertoire complexity in cutaneous T-cell lymphoma. Blood 2003;102:4059–66.
9. Liu HL, Hoppe RT, Kohler S, Harvell JD, Reddy S, Kim YH. CD30+ cutaneous lymphoproliferative disorders: the Stanford experience in lymphomatoid papulosis and primary cutaneous anaplastic large cell lymphoma. J Am Acad Dermatol 2003;49:1049–58.
10. Querfeld C, Rosen ST, Guitart J, Kuzel TM. The spectrum of cutaneous T-cell lymphomas: new insights into biology and therapy. Curr Opin Hematol 2005;12:273–8.
11. Kupper TS, Fuhlbrigge RC. Immune surveillance in the skin: mechanisms and clinical consequences. Nat Rev Immunol 2004;4:211–22.
12. Kunkel EJ, Boisvert J, Murphy K, Vierra MA, Genovese MC, Wardlaw AJ, et al. Expression of the chemokine receptors CCR4, CCR5, and CXCR3 by human tissue-infiltrating lymphocytes. Am J Pathol 2002;160:347–55.
13. Campbell JJ, Haraldsen G, Pan J, Rottman J, Qin S, Ponath P, et al. The chemokine receptor CCR4 in vascular recognition by cutaneous but not intestinal memory T-cells. Nature 1999;400:776–80.
14. Campbell JJ, Clark RA, Watanabe R, Kupper TS. Sezary syndrome and mycosis fungoides arise from distinct T-cell subsets: a biologic rationale for their distinct clinical behaviors. Blood 2010;116:767–71.
15. Wu XS, Lonsdorf AS, Hwang ST. Cutaneous T-cell lymphoma: roles for chemokines and chemokine receptors. J Invest Dermatol 2009;129:1115–9.
16. Tokura Y, Sugita K, Yagi H, Shimauchi T, Kabashima K, Takigawa M. Primary cutaneous anaplastic large cell lymphoma with fatal leukemic outcome in association with CLA and CCR4-negative conversion. J Am Acad Dermatol 2007;57:S92–6.
17. Olkhanud PB, Baatar D, Bodogai M, Hakim F, Gress R, Anderson RL, et al. Breast cancer lung metastasis requires expression of chemokine receptor CCR4 and regulatory T-cells. Cancer Res 2009;69:5996–6004.
18. Curiel TJ, Coukos G, Zou L, Alvarez X, Cheng P, Mottram P, et al. Specific recruitment of regulatory T-cells in ovarian carcinoma fosters immune privilege and predicts reduced survival. Nat Med 2004;10:942–9.
19. Ishida T, Iida S, Akatsuka Y, Ishii T, Miyazaki M, Komatsu H, et al. The CC chemokine receptor 4 as a novel specific molecular target for immunotherapy in adult T-cell leukemia/lymphoma. Clin Cancer Res 2004;10:7529–39.
20. Kadin ME, Cavaille-Coll MW, Gertz R, Massague J, Cheifetz S, George D. Loss of receptors for transforming growth factor beta in human T-cell malignancies. Proc Natl Acad Sci U S A 1994;91:6002–6.
21. Sui J, Li W, Murakami A, Tamin A, Matthews LJ, Wong SK, et al. Potent neutralization of severe acute respiratory syndrome (SARS) coronavirus by a human mAb to S1 protein that blocks receptor association. Proc Natl Acad Sci U S A 2004;101:2536–41.
22. Reff ME, Carner K, Chambers KS, Chinn PC, Leonard JE, Raab R, et al. Depletion of B cells *in vivo* by a chimeric mouse human monoclonal antibody to CD20. Blood 1994;83:435–45.
23. www.rndsystems.com/pdf/fab1567a.pdf
24. Jopling LA, Sabroe I, Andrew DP, Mitchell TJ, Li Y, Hodge MR, et al. The identification, characterization, and distribution of guinea pig CCR4 and epitope mapping of a blocking antibody. J Biol Chem 2002;277:6864–73.

25. Pfeifer W, Levi E, Petrogiannis-Haliotis T, Lehmann L, Wang Z, Kadin ME. A murine xenograft model for human CD30+ anaplastic large cell lymphoma. Successful growth inhibition with an anti-CD30 antibody (HeFi-1). Am J Pathol 1999;155:1353–9.
26. Whitelegg NR, Rees AR. WAM: an improved algorithm for modelling antibodies on the WEB. Protein Eng 2000;13:819–24.
27. Daura X, Oliva B, Querol E, Aviles FX, Tapia O. On the sensitivity of MD trajectories to changes in water-protein interaction parameters: the potato carboxypeptidase inhibitor in water as a test case for the GROMOS force field. Proteins 1996;25:89–103.
28. Carter PJ. Potent antibody therapeutics by design. Nat Rev Immunol 2006;6:343–57.
29. Lazar GA, Dang W, Karki S, Vafa O, Peng JS, Hyun L, et al. Engineered antibody Fc variants with enhanced effector function. Proc Natl Acad Sci U S A 2006;103:4005–10.
30. Baatar D, Olkhanud P, Sumitomo K, Taub D, Gress R, Biragyn A. Human peripheral blood T regulatory cells (Tregs), functionally primed CCR4+ Tregs and unprimed CCR4- Tregs, regulate effector T cells using FasL. J Immunol 2007;178:4891–900.
31. Byrne WL, Mills KH, Lederer JA, O'Sullivan GC. Targeting regulatory T-cells in cancer. Cancer Res 2011;71:6915–20.
32. Hirahara K, Liu L, Clark RA, Yamanaka K, Fuhlbrigge RC, Kupper TS. The majority of human peripheral blood CD4+CD25highFoxp3+ regulatory T-cells bear functional skin-homing receptors. J Immunol 2006;177:4488–94.
33. Ishida T, Ishii T, Inagaki A, Yano H, Kusumoto S, Ri M, et al. The CCR4 as a novel-specific molecular target for immunotherapy in Hodgkin lymphoma. Leukemia 2006;20:2162–8.
34. Niwa R, Shoji-Hosaka E, Sakurada M, Shinkawa T, Uchida K, Nakamura K, et al. Defucosylated chimeric anti-CC chemokine receptor 4 IgG1 with enhanced antibody-dependent cellular cytotoxicity shows potent therapeutic activity to T-cell leukemia and lymphoma. Cancer Res 2004;64:2127–33.
35. Ishida T, Joh T, Uike N, Yamamoto K, Utsunomiya A, Yoshida S, et al. Defucosylated anti-CCR4 monoclonal antibody (KW-0761) for relapsed adult T-cell leukemia-lymphoma: a multicenter phase II study. J Clin Oncol 2012;30:837–42.
36. Yamamoto K, Utsunomiya A, Tobinai K, Tsukasaki K, Uike N, Uozumi K, et al. Phase I study of KW-0761, a defucosylated humanized anti-CCR4 antibody, in relapsed patients with adult T-cell leukemia-lymphoma and peripheral T-cell lymphoma. J Clin Oncol 2010;28:1591–8.
37. Ishida T, Utsunomiya A, Iida S, Inagaki H, Takatsuka Y, Kusumoto S, et al. Clinical significance of CCR4 expression in adult T-cell leukemia/lymphoma: its close association with skin involvement and unfavorable outcome. Clin Cancer Res 2003;9:3625–34.
38. Yano H, Ishida T, Inagaki A, Ishii T, Ding J, Kusumoto S, et al. Defucosylated anti-CC chemokine receptor 4 monoclonal antibody combined with immunomodulatory cytokines: a novel immunotherapy for aggressive/refractory mycosis fungoides and Sezary syndrome. Clin Cancer Res 2007;13:6494–500.
39. Yano H, Ishida T, Imada K, Sakai T, Ishii T, Inagaki A, et al. Augmentation of antitumour activity of defucosylated chimeric anti-CCR4 monoclonal antibody in SCID mouse model of adult T-cell leukaemia/lymphoma using G-CSF. Br J Haematol 2008;140:586–9.
40. Bindon CI, Hale G, Bruggemann M, Waldmann H. Human monoclonal IgG isotypes differ in complement activating function at the level of C4 as well as C1q. J Exp Med 1988;168:127–42.
41. Teeling JL, Mackus WJ, Wiegman LJ, van den Brakel JH, Beers SA, French RR, et al. The biological activity of human CD20 monoclonal antibodies is linked to unique epitopes on CD20. J Immunol 2006;177:362–71.
42. Ong GL, Mattes MJ. Mouse strains with typical mammalian levels of complement activity. J Immunol Methods 1989;125:147–58.
43. Lloyd CM, Delaney T, Nguyen T, Tian J, Martinez AC, Coyle AJ, et al. CC chemokine receptor (CCR)3/eotaxin is followed by CCR4/monocyte-derived chemokine in mediating pulmonary T helper lymphocyte type 2 recruitment after serial antigen challenge *in vivo*. J Exp Med 2000;191:265–74.
44. Ferenczi K, Fuhlbrigge RC, Pinkus J, Pinkus GS, Kupper TS. Increased CCR4 expression in cutaneous T-cell lymphoma. J Invest Dermatol 2002;119:1405–10.
45. Gear AR, Camerini D. Platelet chemokines and chemokine receptors: linking hemostasis, inflammation, and host defense. Microcirculation 2003;10:335–50.
46. Abi-Younes S, Si-Tahar M, Luster AD. The CC chemokines MDC and TARC induce platelet activation via CCR4. Thromb Res 2001;101:279–89.
47. Zou W. Regulatory T-cells, tumour immunity and immunotherapy. Nat Rev Immunol 2006;6:295–307.
48. Hong H, Gu Y, Zhang H, Simon AK, Chen X, Wu C, et al. Depletion of CD4+CD25+ regulatory T cells enhances natural killer T cell-mediated anti-tumour immunity in a murine mammary breast cancer model. Clin Exp Immunol 2010;159:93–9.
49. Watanabe Y, Katou F, Ohtani H, Nakayama T, Yoshie O, Hashimoto K. Tumor-infiltrating lymphocytes, particularly the balance between CD8 (+) T-cells and CCR4(+) regulatory T-cells, affect the survival of patients with oral squamous cell carcinoma. Oral Surg Oral Med Oral Pathol Oral Radiol Endod 2010;109:744–52.
50. Yuan Q, Bromley SK, Means TK, Jones KJ, Hayashi F, Bhan AK, et al. CCR4-dependent regulatory T-cell function in inflammatory bowel disease. J Exp Med 2007;204:1327–34.

Supplementary Material and Methods

Cells

Cf2Th-CCR4, Cf2Th-CCR5, and 293T-CCR4 were established by transfection with full-length CCR4 or CCR5 expressing plasmid and followed by 800 μg/ml and 500 μg/ml G418 selection, respectively, and FACS sorting for CCR^+ cell population. Cells were authenticated by detecting CCR molecules using FACS.

Transfections and Biosynthetic Analyses of human CCR-Fc fusion proteins

Transfections were done with 293 cells and a F105-L3-Nt-hCCR-Fc fusion protein vector using the same method described above. Two days post-transfection, the cells were washed and then incubated for various times with either 250 μCi/ml [^{35}S]Met/Cys or 400 μCi/ml Na_2 $^{35}SO_4$ (PerkinElmer Life Sciences, MA). After two days, culture supernatant was collected and prepared for immunoprecipitation using Protein A sepharose beads. The purified hCCR-Fc fusion proteins, i.e. hCCR4Nt-Fc, hCCR5Nt-Fc and mutant hCCR5Nt-Fc (with four N-terminal tyrosine residues mutated to aspartic acid, DDDD mutant version), were further analyzd by SDS-PAGE and silver staining.

Sandwich enzyme-linked immunosorbent assay (ELISA)

The 96-well plates were coated with mAb1567 antibody in 50 mM carbonate buffer (pH 9.6) at 4 °C overnight, and the wells were washed five times with PBST (PBS containing 0.2% Tween-20), followed by incubation with 200 µl of blocking buffer (PBS, pH 7.4, containing 5% sucrose and 1% BSA) at 37°C for 2 h. Human CCRNt-Fc fusion proteins were added at concentration of 0.25, 0.5 or 1 µg per well and then incubated at 4°C for 1 h. After washing PBST, the horseradish peroxidase (HRP) labeled goat anti-human IgG (Thermo scientific, IL) was added into wells and then incubated for 1 h at 4°C. The plates were then washed and incubated with TMB substrate solution (KPL, MD) at room temperature in the dark. The reaction was stopped by the addition of 0.6N sulfuric acid and the absorbance determined at 450 nm with a microplate reader.

Construction of humanized 1567 light-chain shuffling phage display library

VH (Variable region of heavy chain) gene of humanized 1567, inparticular HCDR3, was cloned as a NcoI/BspEI fragment into the vector pFarber-Vκ-rep which contains a repertoire of 1.2 x 10^8 non-immune Vκ genes derived from 57 healthy donors. Ligated DNA was transformed into eclectroporation-competent *E. Coli.* TG1 cells following manufacturer's instructions (Stratagene, CA). Multiple transformations were performed to generate the h1567-Vk chain shuffled library at desired size close to that of the Vκ repertoire.

Cloning and construction of MAB1567 gene from hybridoma cell line

Briefly, total RNA was extracted from hybridoma cells MAB1567 (R&D systems) using Total RNA Purification Kit (Ambio Inc., TX) and then reverse transcribed to cDNAs using manufacturer's protocol (Promega) and AMV reverse transcriptase (Promega). The cDNAs of VH and VL antibody fragments were subsequently amplified by PCR with degenerative primers specific for mouse antibody V regions and the full length scFvs (VH-$(G_4S)_3$ linker-VL) was assembled by PCR according the manufacture's protocol (GE-Pharmacia Biotech). For antibody production, the constructed scFv-Fc in pcDNA3.1-Hinge vector (murine scFv in frame with the C-terminal human IgG1 Fc) and IgG1 in TCAE5.3 vector were transiently transfected into 293T or 293F cells, and the secreted antibodies in the cell culture supernatants were purified by Protein A affinity chromatography.

Construction of h1567 phage display random mutagenesis library

At the selected six CDR positions, all 20 amino acids except proline, cysteine or methionine were allowed at each position to be totally randomized at equal frequency. The full scFv fragments were *de novo* synthesized to carry these mutations at the designated positions by Sloning Biotech. The synthesized scFv fragment library was sample sequenced to confirm the

mutation frequency and accuracy. The library was constructed by subcloning the synthesized scFv library into phage display vector pFarber by electroporation of *E. Coli.* TG1 cells following manufacturer's instructions (Stratagene, CA).

Library selection and screening

CCR4-PMPL preparation for phage antibody library selection, library selection with CCR4-PMPLs or $CCR4^+$ Mac-1 cells, FACS screening for positive binder, DNA sequencing and sequence analysis were performed following the procedure described previously (1-3).

Regulatory T cell suppression assay

$CD4^+CD25^{high}$ and $CD4^+CD25^-$ T cells were obtained as previous described. $CD4^+CD25^-$ Teffs (1×10^4 cells) were stained by CFSE (Invitrogen) and then cultured with $CD4^+CD25^{high}$ Tregs (1×10^3 cells) in round-bottom 96-well Costar plates coated with 0.05 μg/ml plate-bound anti-CD3 (clone UCHT1) and 1 μg/ml soluble anti-CD28 (clone CD28.2) antibodies (BD Pharmigen). Anti-CCR4 antibodies, c1567IgG and Ab2-3IgG, and control IgG were added and incubated for 3 and 7 days and then analyzed by counting beads and flow cytometry.

Reference

1. Mirzabekov T, Kontos H, Farzan M, Marasco W, Sodroski J. Paramagnetic proteoliposomes containing a pure, native, and oriented seven-transmembrane segment protein, CCR5. Nat Biotechnol. 2000;18:649-54.

2. Sui J, Aird DR, Tamin A, Murakami A, Yan M, Yammanuru A, et al. Broadening of neutralization activity to directly block a dominant antibody-driven SARS-coronavirus evolution pathway. PLoS Pathog. 2008;4:e1000197.

3. Xu C, Sui J, Tao H, Zhu Q, Marasco WA. Human anti-CXCR4 antibodies undergo VH replacement, exhibit functional V-region sulfation, and define CXCR4 antigenic heterogeneity. J Immunol. 2007;179:2408-18.

Supplementary Figure 1

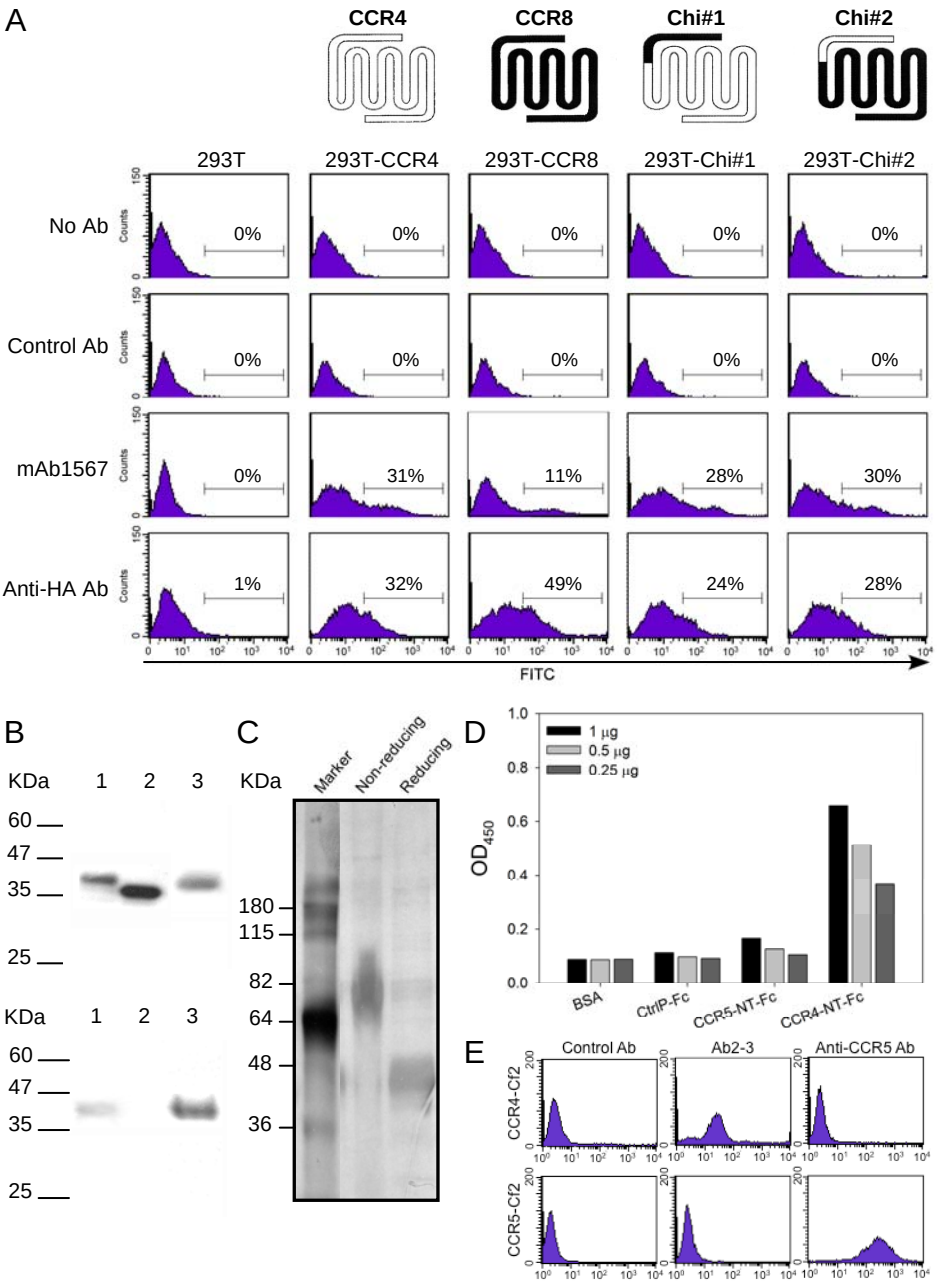

Supplementary Figure 2

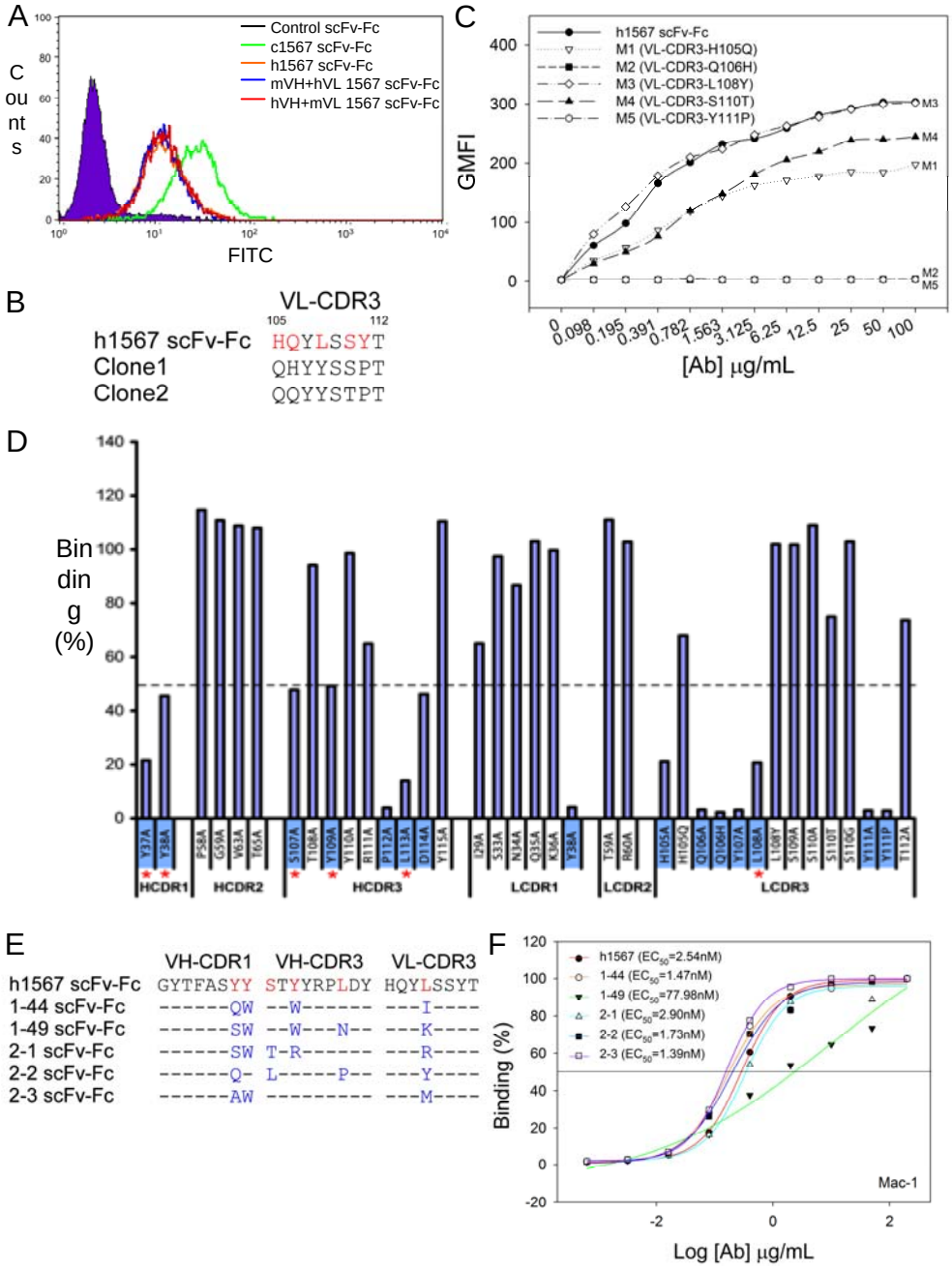

Supplementary Figure 3

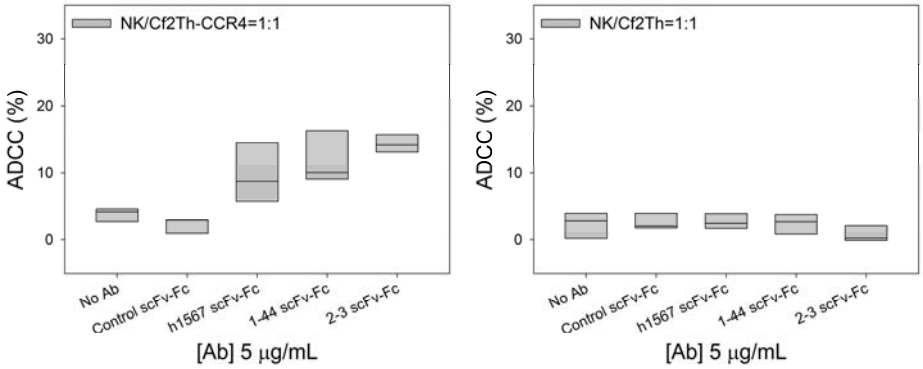

Supplementary Figure 4

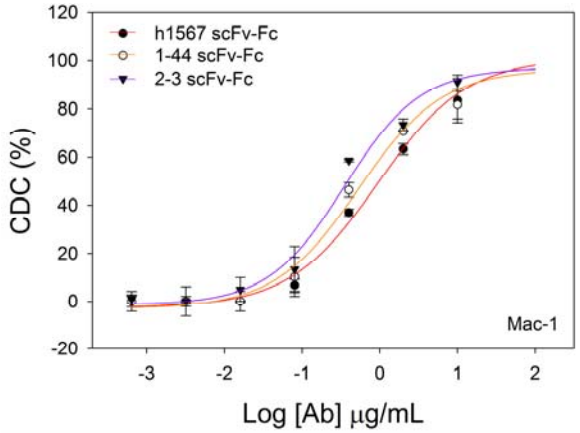

Supplementary Figure 5

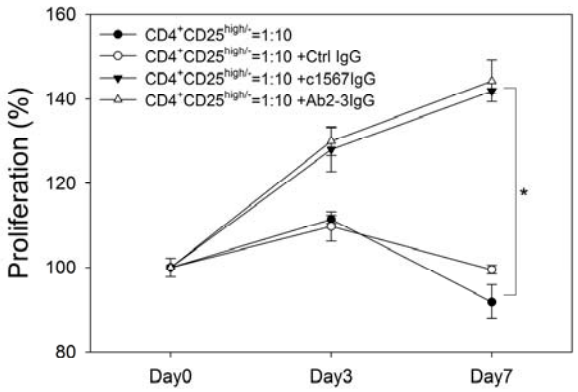

Supplementary Figures

Supplementary Fig. S1. Epitope mapping of mAb1567. *A*, The NH_2-terminal extracellular domains of human CCR4 and CCR8 were swapped as indicated and designated as Chimera #1 and #2 (Chi#1 and Chi#2). The chimeras as well wild type human CCR4 and CCR8 were transiently transfected into 293T cells and tested for binding with murine mAb1567. Similar level of surface expression of these receptors was validated by detecting the N-terminal haemagglutinin (HA) tag using anti-HA antibody. *B*, Expression of human CCR4 N-terminal with Fc domain fusion protein (CCR4Nt-Fc). 293T cells expressing hCCR4Nt-Fc fusion protein were labeled with [^{35}S]-cysteine and [^{35}S]-methionine (upper panel) or [^{35}S]-sulfate (lower panel). Culture supernatant containing secreted proteins were immunoprecipitated with protein A sepharose beads and applied to SDS-PAGE reducing gel for analysis. Lane 1 and 2, wt or DDDD mutant version of CCR5Nt-Fc where 4Y's at positions 3, 10, 14 and 15 which undergo tyrosine sulfation are changed to D; lane 3, wt CCR4Nt-Fc. The lower panel shows tyrosine sulfation of Nt-tyrosine residues in CCR5-Nt (lane 1) and CCR4-Nt (lane 3) but not the CCR5-Nt DDDD mutant (lane 2). *C*, Silver staining of secreted CCR4Nt-Fc on non-reducing and reducing gel showed the presence of dimeric and monomeric protein, respectively. *D*, Three different fusion proteins, control protein-Fc (CtrlP-Fc), CCR5Nt-Fc and CCR4Nt-Fc, and Bovine serum albumin (BSA) were tested the binding ability to mAb1567 at three different concentrations (0.25, 0.5 or

1 μg per well) and detected by HRP-anti-human Fc IgG using an ELISA reader. *E*, CCR4 or CCR5 expressed Cf2 cells were stained by either anti-CCR4 or anti-CCR5 antibodies and analyzed by using flow cytometry.

Supplementary Fig. S2. Affinity maturation of humanized anti-CCR4 mAb1567. *A*, Binding activity comparison among chimeric, humanized and mouse/human VH and VK hybrid 1567 antibodies. Both mouse heavy chain-human light chain (mVH+hVL 1567 scFv-Fc, blue line) and human heavy chain-mouse light chain (hVH+mVL 1567 scFv-Fc, red line) showed similar affinity as h1567 scFv-Fc (orange line) but weaker than parental c1567 at 0.1 μg/ml, an Ab concentration that can discriminate binding affinities. The VL of Ab1567 played an equally important role as the VH in recognizing CCR4. *B*, By sequencing 48 randomly picked non-binding Ab clones from the unselected VL shuffled library, two sequences was found to have the same VL sequence as h1567 except for five residues in the CDR3. Amino acid number based on the IMGT database numbering scheme is shown on the top. *C*, Mutations in VL-CDR3 effecting 1567's binding to CCR4. Further mutagenesis on these singly selected residues showed that mutant M3 (L108Y) retained full binding activity whereas M1 (H105Q) and M4 (S110T) had moderate loss of binding activity and mutants M2 (Q106H) and M5 (Y111P) had complete loss of binding. The VL and in particular the four residues (H105, Q106, S110 and Y111) in the VL-

CDR3 are critically important for binding to CCR4. *D*, Alanine-scanning analysis of residues in the CDRs of h1567 for binding to CCR4 on Mac-1 cells. As the VL played an equally important role as VH in CCR4 binding, all the CDRs in both VH and VL were included in the mutagenesis study (total of 31 residues) to assess the specific contribution of each CDR residue to CCR4 binding. A few non-alanine mutants in VL-CDR3 were also included in the analysis. Binding percentage of each mutant was normalized against wild type humanized mAb1567 scFv-Fc (100%) and mutant Abs were all tested at concentration of 3.7 μg/ml. Total 13 residues (highlighted in blue) in four CDRs (VH-CDR1 (HCDR1), VL-CDR1 (LCDR1), HCDR3 and LCDR3) reduced more than 50% binding activity. Further analysis of the 13 residues in their possible roles for maintaining CDR3 loop canonical structures showed that seven residues might act as "scaffolding" residues (HCDR3-P112, HCDR3-D114, LCDR1-Y38, LCDR3-H105, LCDR3-Q106, LCDR3-Y107 and LCDR3-Y111). To maintain the structural integrity of the antigen-binding site, these seven amino acids were kept as wild type. The other six amino acids were chosen to be randomized (red asterisks) and a mutant h1567-Ab phage-display library with a diversity of 4.1×10^7 was constructed for affinity optimization. *E*, Amino acid sequence alignment of humanized mAb1567 and mAb binding variants with associated VH-CDR1, VH-CDR3 and VL-CDR3 amino acid differences among them. After panning against Mac-1 cells, five unique h1567 phage-scFv variants that bound strongly were identified. *F*, Dose dependent

binding curve of humanized 1567 and it's variants to $CCR4^+$ Mac-1 cells by FACS analysis. Binding percentage shown on Y-axis of each variant was normalized against h1567 scFv-Fc (100%). Three out of the five, 2-2, 1-44 and 2-3, showed higher binding activity to Mac-1 cells than parental h1567 with EC_{50} of 1.73, 1.47, and 1.39 nM, respectively.

Supplementary Fig. S3. Human mAb1567 variants mediated ADCC activity against Cf2-CCR4 cells via human NK cells. Antibodies were tested at concentration of 5 μg/mL, NK cell to target cells ratio was at 1:1. Data are shown in a box and whiskers graph and represent three independent experiments and each was performed with NK cells from a different health donor; the box extends from lowest percentile to the highest percentile, with a line at the median. The whiskers above and below the box indicate the 95th and 5th percentiles. Left panel, Cf2-CCR4 cells; right panel, control Cf2 cells.

Supplementary Fig. S4. CDC activity of h1567, 1-44 and 2-3 variants against Mac-1 cells.

Supplementary Fig. S5. Anti-CCR4 antibodies abrogate the suppressive function of Tregs on Teff proliferation. $CD4^+CD25^-$ T cells were CFSE-labeled, incubated with Tregs at 10:1 ratio, and then stimulated with anti-CCR4 antibodies and control antibody in the presence of

anti-CD3/28 co-stimulation. After 3 and 7 days cells were harvested and analyzed by flow cytometry. The percentage of cells was calculated among the fluorescence positive $CD4^{+}CD25^{-}$ T and counting beads. The percent proliferation was normalized to $CD4^{+}CD25^{-}$ T effector cells at Day 0. The data shown were calculated from two independent experiments. Bars represent mean ± S.D.. "*" indicates $p < 0.05$.